

See discussions, stats, and author profiles for this publication at: <https://www.researchgate.net/publication/235421361>

# Chemoaffinity Material for Plasmid DNA Analysis by High-Performance Liquid Chromatography with Condition-Dependent Switching between Isoform and Topoisomer Selectivity

ARTICLE in ANALYTICAL CHEMISTRY · FEBRUARY 2013

Impact Factor: 5.64 · DOI: 10.1021/ac3034823 · Source: PubMed

---

CITATIONS

7

---

READS

60

5 AUTHORS, INCLUDING:



**Marek Mahut**

University of Vienna

11 PUBLICATIONS 62 CITATIONS

SEE PROFILE



**Andrea Gargano**

University of Amsterdam

13 PUBLICATIONS 126 CITATIONS

SEE PROFILE



**Wolfgang Lindner**

University of Vienna

269 PUBLICATIONS 7,044 CITATIONS

SEE PROFILE

# Chemoaffinity Material for Plasmid DNA Analysis by High-Performance Liquid Chromatography with Condition-Dependent Switching between Isoform and Topoisomer Selectivity

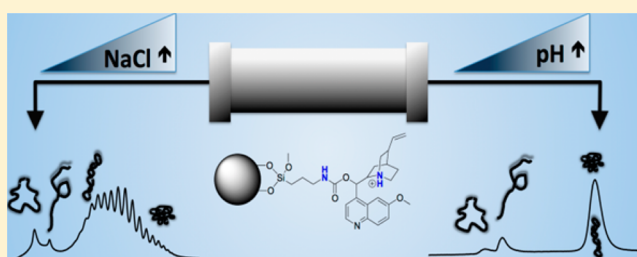
Marek Mahut,<sup>†</sup> Andrea Gargano,<sup>†</sup> Hermann Schuchnigg,<sup>‡</sup> Wolfgang Lindner,<sup>†</sup> and Michael Lämmerhofer<sup>\*,†</sup>

<sup>†</sup>Institute of Analytical Chemistry, University of Vienna, Währinger Strasse 38, A-1090 Vienna, Austria

<sup>‡</sup>Boehringer Ingelheim RCV GmbH & Co KG, Dr.- Böhringer-Gasse 5-11, A-1120 Vienna, Austria

## S Supporting Information

**ABSTRACT:** Plasmid DNA may exist in three isoforms, the linear, open-circular (oc, “nicked”), and covalently closed circular (ccc, “supercoiled”) form. We have recently reported on the chromatographic separation of supercoiled plasmid topoisomers on cinchona-alkaloid modified silica-based stationary phases. Herein, we present a selectivity switching mechanism to achieve separation of isoforms and/or supercoiled topoisomers using the very same chromatographic column and system. While salt gradient elution facilitates topoisomer separation, the supercoiled species are eluting as a single peak upon elution by a mixed pH and organic modifier gradient, still well separated from the other isoforms. We have found that a mobile phase pH value near the *pI* of the zwitterionic adsorbent surface leads to full recovery of all plasmid DNA isoforms, which is a major issue when using anion exchange-based resins. Furthermore, the observed elution pattern, oc < linear < ccc, is constant upon changes of mobile phase composition, gradient slope, and plasmid size. The remarkable isoform selectivity found on quinine-based selectors is explained by van’t Hoff plots, revealing a different binding mechanism between the supercoiled plasmid on one hand and the oc and linear isoforms on the other hand.



Plasmid DNA (pDNA) is an extrachromosomal genetic unit providing its host cell with additional functionalities, and since the discovery of the great potential for its use as a genetic therapeutic, much attention is paid to these novel types of drugs.<sup>1</sup> In November 2012, the first drug for gene therapy has been approved by the European Medicines Agency,<sup>2</sup> which may mark a new therapeutic era, as there are numerous other genetic agents in clinical phases covering a broad range of health issues. The key element bearing the correct gene is the plasmid DNA (or the derived RNA), which to date is most often packed into adeno-associated virus particles.<sup>3</sup> From three possible isoforms, the so-called covalently closed circular (ccc) form is considered to be most active for therapeutics. Pharmaceutical grade ccc pDNA is produced by fermentation in *Escherichia coli* and isolated subsequently from harvested cells by alkaline cell lysis and multistep purification of pDNA.<sup>4</sup> The final formulation should have a high content of the ccc form relative to other pDNA isoforms (Figure 1a,b), i.e., the linear (lin) and the open circular (oc) isoform.<sup>5</sup> Generally, there is great demand for a reliable analysis of the isoform distribution during in-process and quality control because the other isoforms may be degradation products of the ccc isoform. The oc isoform is obtained from the ccc form by a single nick in the DNA backbone, and the linear form may be formed when two nicks are in close vicinity. Capillary gel electro-

phoresis offers the highest resolving power for such types of analytes<sup>6</sup> but suffers from low robustness and low sample salt-tolerance and is time-consuming, thus methods based on liquid chromatography may be preferred. On the analytical scale, the choice is restrained to anion exchange columns, such as the DNA-NPR from Tosoh Bioscience or GenPak FAX from Waters, both employing nonporous 2.5  $\mu\text{m}$  particles composed of a hydrophilic organic polymer with diethylaminoethyl (DEAE)-based ligands. Such charged organic particles have also been successfully tested for preparative applications,<sup>7</sup> although organomonolithic materials seem to be very promising.<sup>8,9</sup>

Chromatographic ligands are rather unspecific, based on simple tertiary (such as DEAE) or quaternary (such as Q) amines<sup>10</sup> and separate nucleic acids according to the number of negative charges.<sup>11</sup> When analytes differ by tertiary structure but bear the same net charge, such as pDNA isoforms, the separation depends on charge density and hydrodynamic factors.<sup>12</sup> This leads to effects similar to slalom chromatography and cause the isoform separation to be dependent on flow-rate and gradient slope.<sup>13</sup> In preparative chromatography, several

Received: December 10, 2012

Accepted: February 7, 2013

Published: February 7, 2013

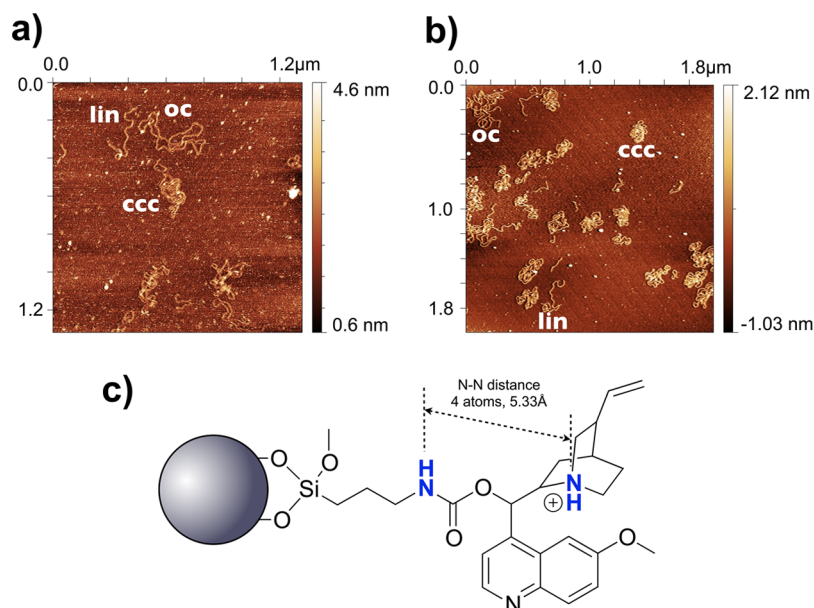


**Figure 1.** (a, b) AFM images of a natural pMCP1 plasmid sample (4.9 kbp) immobilized on amino-modified mica containing all three isoforms in a single image. (c) Structure of the stationary phase with a quinine carbamate ligand used throughout the plasmid DNA separation study. One of the most important structural motifs is the presence of the tertiary amine along with the amide group with a specific distance of 4 atoms between the two nitrogens (5.333 Å, the distance between the two N–H hydrogens is 5.825 Å, taking into account the preferred “anti-open” conformation<sup>39,40</sup>).

small-molecule ligands were investigated<sup>14</sup> that were able to separate the supercoiled from the oc isoform, which is a very challenging impurity,<sup>15</sup> or nucleic acids in general.<sup>16</sup> We chose to employ a quinine carbamate ligand on the analytical scale (see Figure 1c), which is able to form defined interactions with the analytes,<sup>17</sup> leading to predictable elution properties (Figure 1c). Recently, we have employed such a column for separation of topoisomers of the ccc pDNA, i.e., differently supercoiled plasmids. Here we report, that by choosing appropriate mobile phase conditions, the separation mechanism of the column can be switched toward isoform separation with excellent separation properties.

## MATERIALS AND METHODS

HPLC analyses were carried out on an Agilent 1200 SL system (Waldbronn, Germany) equipped with a binary pump, a thermostatted autosampler (cooled to 4 °C), and a DAD UV detector. Prior to analysis, all solvents were 0.22 μm-filtered and ultrasonically degassed. Chromatographic conditions are given in the text, and the synthesis of the stationary phase is given in the Supporting Information. pMCP1 (4.9 kbp, 2.8 mg/mL) plasmid DNA preparations in Tris-EDTA buffer were provided and characterized<sup>18</sup> by Boehringer-Ingelheim RCV (Vienna, Austria), with homogeneities (ccc form contents) > 90%. The oc isoform (50 μg/mL) was produced enzymatically with a nicking endonuclease Nt.BstNBI,<sup>19</sup> purchased from New England Biolabs (Ipswich, MA). The linear isoform (50 μg/mL, produced with an endonuclease) was supplied by Boehringer-Ingelheim RCV. Atomic force microscopy (AFM) images were recorded as described earlier.<sup>20</sup>

## RESULTS AND DISCUSSION

**WAX-Supported Chemoaffinity Principle.** The quinine-carbamate based stationary phase (see Figure 1c) represents a weak anion-exchanger (WAX), and therefore elution of anionic samples like pDNA by a salt (i.e., counterion) gradient is the first choice. A typical chromatogram of a pDNA sample using

NaCl gradient elution can be seen in Figure 2a. The elution order, when using a salt gradient is as follows: oc, linear, and

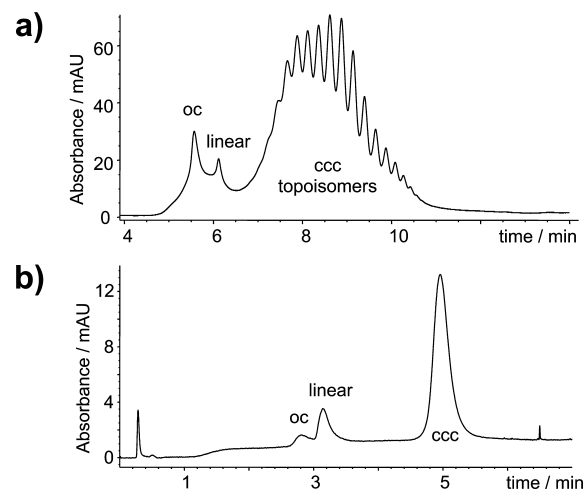


**Figure 2.** Chromatograms of a 4.9 kbp pMCP1 plasmid sample (spiked with linear isoform and with an oc isoform obtained by thermal stress) obtained with a 33 mm × 4.6 mm column employing a quinine carbamate ligand on 1.5 μm nonporous silica, using a NaCl-gradient (a) and a pH-gradient (b). Conditions: (a) buffer A, 50 mM sodium phosphate pH 7.0; buffer B, buffer A + 0.6 M NaCl + 20% (v/v) isopropanol, 60 °C, 0.7 mL/min, 10–35% B in 15 min, 9 μg of pDNA injected; (b) buffer A, 50 mM sodium phosphate pH 7.0; B, 50 mM sodium phosphate pH 7.6 + 20% (v/v) isopropanol, 60 °C, 1.0 mL/min, 0–75% B in 7.5 min, 15 μg of pDNA injected.

ccc isoforms starting with the least supercoiled topoisomer and stronger retention the higher the supercoiling.<sup>21</sup> This order was found to be insensitive to the gradient time ( $t_G$  = 15–120 min), flow rate ( $F$  = 0.3–1.0 mL/min), salt ( $c_{\text{NaCl}}$  = 50–1000 mM NaCl), buffer concentration ( $c_{\text{tot}}$  = 10–100 mM phosphate), modifier content ( $\phi_{\text{isopropanol}}$  = 0–30%), buffer pH value (pH = 6.0–7.7), plasmid size ( $N$  = 2.7–14.5 kbp), and column length

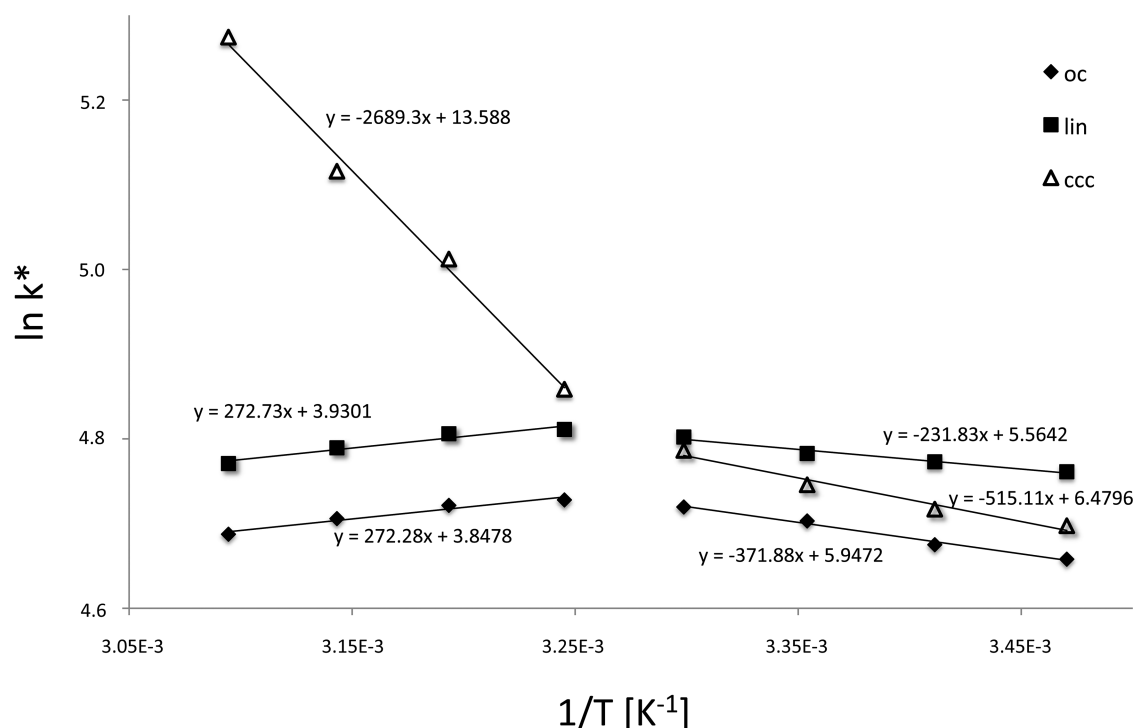


**Figure 3.** van't Hoff Plots of pMCP1 plasmid isoforms on a 33 mm × 4.6 mm column employing a quinine carbamate ligand on 1.5  $\mu$ m nonporous silica. Chromatograms were recorded using a spiked sample containing all three isoforms. Conditions ( $T$  was varied from 15 to 50 °C): buffer A, 50 mM sodium phosphate pH 6.0; buffer B, buffer A + 0.6 M NaCl, 0–100% B in 15 min, 0.9 mL/min, 3  $\mu$ g of pDNA injected.

**Table 1.** Linear Correlation Coefficients and Thermodynamical Data of Plasmid Isoform Separation Calculated from the van't Hoff Plots of Figure 3<sup>a</sup>

isoform	low-temperature range (15–30 °C)			high-temperature range (35–50 °C)		
	oc	linear	ccc	oc	linear	ccc
determination coefficient $R^2$	0.989	0.972	0.970	0.955	0.944	0.994
enthalpy, $\Delta H^\circ$ [kJ/mol]	$3.1 \pm 0.2$	$1.9 \pm 0.2$	$4.3 \pm 0.5$	$-2.3 \pm 0.3$	$-2.3 \pm 0.4$	$22.4 \pm 1.3$
entropy, $\Delta S^\circ$ [J/(mol K)]	$47.2 \pm 1.5$	$44.0 \pm 1.5$	$51.6 \pm 0.5$	$29.7 \pm 1.2$	$30.4 \pm 1.1$	$110.7 \pm 1.7$
$\Delta S^\circ T$ [kJ/mol]	$14.1 \pm 0.4^b$	$13.1 \pm 0.5^b$	$15.4 \pm 0.1^b$	$9.6 \pm 0.4^c$	$9.8 \pm 0.3^c$	$35.8 \pm 0.6^c$
free energy, $\Delta G^\circ$ [kJ/mol]	$-11.0 \pm 0.2^b$	$-11.2 \pm 0.2^b$	$-11.1 \pm 0.4^b$	$-11.9 \pm 0.0^c$	$-12.1 \pm 0.1^c$	$-13.4 \pm 1.8^c$

<sup>a</sup>Chromatographic conditions: buffer A, 50 mM sodium phosphate pH 6.0; buffer B, buffer A + 0.6 M NaCl; gradient, 0–100% B, gradient time ( $t_G$ ), 15 min; flow, 0.9 mL/min;  $t_0$  = 0.26 min;  $t_D$  = 1.10 min (dwell time);  $\phi$  = 1.32 (stationary-to-mobile phase ratio). Gradient retention factor ( $k^*$ ) was calculated using the Linear-Solvent-Strength model from two initial runs at  $t_G$  = 15 and 30 min. <sup>b</sup>Calculated at 25 °C. <sup>c</sup>Calculated at 50 °C.

( $L$  = 5–15 cm) (the numbers in the parentheses represent the tested range). This persistence of elution order is due to specific interaction of pDNA isoforms via simultaneous multiple contacts with the chemoaffinity ligand allowing selective geometrically constrained recognition of individual pDNA forms (see Figure 1c for binding sites).<sup>17</sup> For comparison, the elution order varies with the gradient slope and plasmid size on a commercial and frequently used DNA-NPR column (Tosoh Bioscience, see the Supporting Information for chromatograms), containing a DEAE ligand.<sup>13</sup> On the quinine carbamate phase, the elution order remains unchanged even if the elution conditions (except for temperature) and the separation mode are changed. In this context, Figure 2b represents a chromatogram recorded under elution by a pH gradient that shows a lack of topoisomer selectivity but the same isoform elution order. The corresponding separation mode will be explained in more detail in the following sections.

**Temperature Effects.** Temperature ( $T$ ) has a great impact on the isoform selectivity, and while oc and linear isoforms reveal similar trends in terms of retention time shifts with

temperature changes, the supercoiled isoform behaves differently. Overall, it has to be pointed out that pDNA is subject to a dynamic behavior during separation as it may adopt distinct conformations during chromatography and stationary phase contacts, yet the individual isoforms and topoisomers retain their identity in terms of topology even when temperature changes. Figure 2a was recorded at an elevated temperature of 60 °C. Only at such higher temperatures ( $T \geq 35$  °C up to 70 °C, the highest temperature tested), the ccc isoform elutes after the linear isoform and hence the elution order described in the previous section is valid, while below 25 °C (with all other parameters identical), the ccc isoform elutes between oc and linear isoforms and completely coelutes with the linear isoform at 30 °C (data not shown). By increasing  $T$ , retention of the ccc isoform increased dramatically, while those of the other isoforms remained similar. In order to understand the thermodynamics behind this process, we have run separations of a pDNA sample containing all three isoforms between 15 and 50 °C. Then we calculated the gradient retention factors ( $k^*$ ) from the peak apex retention times<sup>22</sup> (i.e., isocratic



retention factors derived from gradient runs) and plotted their natural logarithms against the reciprocal absolute temperature in form of a van't Hoff plot according to eq 1

$$\ln k^* = -\frac{1}{T} \frac{\Delta H^\circ}{R} + \frac{\Delta S^\circ}{R} \ln \phi \quad (1)$$

wherein  $T$  is the absolute temperature (in K),  $R$  is the gas constant,  $\Delta H^\circ$  and  $\Delta S^\circ$  are enthalpy and entropy change upon transfer from mobile to stationary phase, and  $\phi$  is the phase ratio (i.e., of volume of stationary to mobile phase  $V_s/V_m$ ).

The highest selectivity between ccc and linear as well as oc isoform is found at high temperatures (Figure 3). Furthermore, it is striking that van't Hoff plots are nonlinear, i.e., the mechanism of adsorption changes with temperature. The temperature range can be visually divided into two sections, a lower range (15–30 °C) and a higher range (35–50 °C), each showing a linear behavior (bilinear van't Hoff plots). The thermodynamical values for both sections and each isoform are given in Table 1. In all cases, the transfer of the pDNA isoforms from the mobile to the stationary phase is an exergonic process, which was expected given the large  $k^*$ -values above 40. The comparison of enthalpic ( $\Delta H^\circ$ ) and entropic contributions ( $T\Delta S^\circ$ ) to Gibbs free energy shows that the retention process is driven entropically in all cases. The large entropy values (relative to enthalpy values) indicate a substantial amount of solvate shell being released upon interaction with the stationary phase. As would be expected, like in hydrophobic interaction chromatography,<sup>23</sup> the entropy change upon adsorption of the oc and linear isoforms decrease with increasing temperature due to a higher mobility of the (solvate shell) molecules. However, the entropy change of the ccc isoform is more than doubled in the higher temperature range (50 °C) compared to the lower temperature range (25 °C). Further, the binding process of the oc and linear isoforms is exothermic at elevated temperatures whereas it is endothermic in the lower temperature range. Because of the different behavior of the ccc isoform in this regard, where the enthalpy change is increased 5-fold at elevated temperature, we argue that a certain molecular rearrangement takes place, probably leading to a larger exposure of the DNA-helix grooves. This rearrangement itself would consume a larger energy portion in the case of the ccc isoform (higher, positive  $\Delta H^\circ$ ), which is very compact due to its high supercoiling, but would release even more energy due to the entropic gain upon lowering the compactness (liberation of counterions and solvation shell may lead to stronger electrostatic repulsion and reduction of compactness). The oc and linear isoforms do not have any supercoiling and consequently they should behave differently.

The peak width of the ccc isoform at 15 °C is about 2 times broader than that of the other two isoforms (fwhm 0.7 min (ccc), 0.3 min (oc/lin)). Interestingly, at 30 °C the peak width of the ccc form increased. At first glance, this contradicts the chromatographic theory, where higher temperature causes a decrease in the C-term of the van Deemter equation leading to narrower peaks, which is the case for the other two isoforms (fwhm 0.8 (ccc), 0.2 min oc/lin)). However, the observed effect is caused by increasing topoisomer selectivity, and at temperatures above 40 °C individual topoisomer peaks can be seen. In Figure 4a, the temperature-dependent topoisomer peak patterns are plotted next to each other and not in real time scale for clearer demonstration (see the Supporting Information for retention times). It can be seen, that the topoisomer selectivity is heavily dependent on temperature and that the

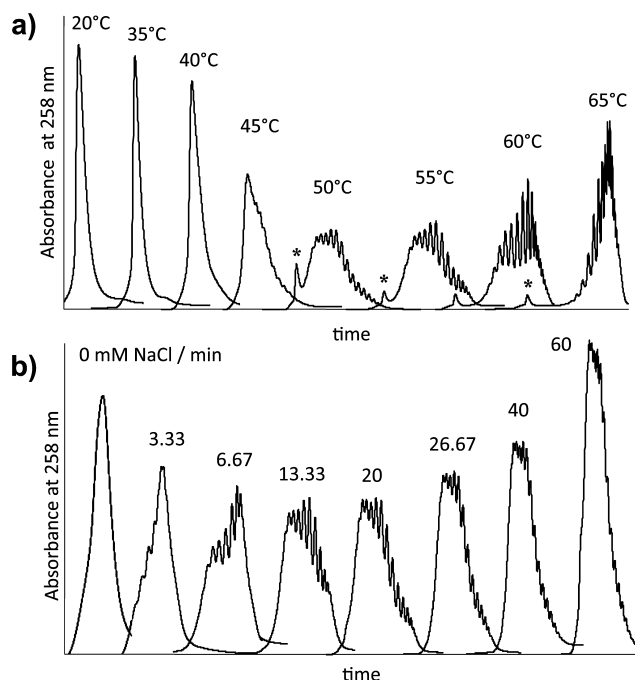


**Figure 4.** Peaks of the ccc isoform from chromatograms recorded at different temperatures (a) and different salt gradients (b) on a 33 mm  $\times$  4.6 mm column employing a quinine carbamate ligand on 1.5  $\mu$ m nonporous silica. Peaks were arranged in parallel for easier interpretation and do not reflect the actual retention times (see the Supporting Information). The asterisk denotes the open circular isoform. Note that the peak shapes recorded at lower temperatures correspond to the shapes at higher salt gradients and vice versa. Conditions: (a) buffer A, 50 mM sodium phosphate pH 7.0; buffer B, buffer A + 0.6 M NaCl + 30% IPA, 0–100% B in 15 min, 0.7 mL/min, 9  $\mu$ g of pDNA injected,  $T$  = 20, 35, 40, 45, 50, 55, 60, and 65 °C. (b) Buffer A, 50 mM sodium phosphate pH 7.0; buffer B, buffer A + “x” M NaCl + 30% IPA, 0–100% B in 15 min, 50 °C, 0.7 mL/min, 9  $\mu$ g of pDNA injected, “x” = 50, 100, 200, 300, 400, 600, and 900 mM NaCl.

maximum selectivity is reached at 60 °C, which is still below the melting temperature of this pDNA sample.<sup>21</sup> Although individual topoisomer peaks are not distinguishable at  $T$  < 40 °C, we assume that a minor (unresolved) topoisomer selectivity is responsible for larger peak widths of the ccc peak compared to oc and linear isoforms.

**Ionic Strength Effects.** In this regard, the results of another study, where the salt concentration in buffer B (0–900 mM NaCl) and thus the slope of the sodium chloride gradient (0–60 mM NaCl/min) was varied, provide complementary results ( $T$  = 50 °C). The resulting peak patterns in Figure 4b have been plotted next to each other to clearly demonstrate the correlation to the temperature study (see the Supporting Information for retention times). With no NaCl present in buffer B, the ccc isoform elutes as a single peak with no topoisomer selectivity. In this case, the plasmid DNA is eluted by the isopropanol gradient only (note that the volume fraction of isopropanol in buffer B has been increased to 30% (v/v) in this study). In all cases where NaCl is present, however, individual topoisomers can be recognized.

From the peak apex retention time of the most abundant topoisomer, which is invariant in a pDNA sample, the NaCl concentration at the point of elution has been calculated (see Figure 4b). Unexpectedly, when comparing peak patterns in Figure 4a,b, the patterns recorded at lower temperature

correspond well to those recorded at higher NaCl concentration and *vice versa*. It is worth noting that the topoisomers' concentration in the sample solution is invariant (data given in Table S4 in the Supporting Information), and thus plasmid structure is only affected by mobile phase conditions. Along that line, Studdert et al. have described that lowering the temperature and increasing the salt concentration has the same qualitative effect on the circular dichroism (CD) spectra of double-stranded DNA.<sup>24</sup> Following their data, such a behavior might be explained by the change of twist with variation of temperature and ionic strength (i.e., counterion concentration with regards to phosphates).<sup>25</sup> It is known that a temperature increase leads to unwinding of the DNA double helix and thus to an increase in the helical repeat and decrease of the twist, respectively.<sup>26,27</sup> On the other hand, repulsion between negative charges of phosphate backbone tends to unwind the DNA helix. Consequently an increase of the sodium ions (i.e., counterions in general) will lead to a decrease of repulsion, and the helix gets more tightly wound. The helical repeat decreases and thus the twist increases. This leads also to a compaction of the DNA molecule.

When following the thermodynamic observations of Studdert et al., it appears that the solvation of the vicinity of phosphates is an equally important factor and may be modified by changing the counterion type and concentration or by changing the dielectric constant (e.g., when adding an organic modifier). However, as we pointed out, such change may lead automatically to a change in DNA twist. Thus, it is unclear, whether a change in twist or a change in solvation is the specific, dominating factor here for variation of retention with change of experimental conditions (such as temperature and NaCl concentration) but it is likely an interplay of both effects. Nevertheless, the present chromatographic behavior indicates a major change in the solvate shell of the analyte upon binding to the stationary phase and complements the thermodynamical observations. Additionally, the plot of the reciprocal NaCl concentration at the point of elution against the logarithm of the gradient retention factor ( $\log k^*$ ) of the ccc form also shows two separate linear ranges (see Figure S4 in the Supporting Information). The slopes in such plots are, according to the stoichiometric displacement model,<sup>28</sup>

$$\log k^* = 2Z \log(1/[\text{NaCl}]) + \log K_z \quad (2)$$

directly proportional to the number of charges that are involved in the ion-exchange process, wherein the slope  $Z$  is related to the ratio of the effective charge number accessible at the analyte (here  $z_{\text{eff}}$  pDNA) and the counterion (here  $z$  of chloride).<sup>29</sup> The intercept  $\log K_z$  is dependent on the ion-exchange equilibrium constant, the surface charge density of the ion-exchanger, the specific surface area, and the mobile phase volume. Since the effective charge number  $z$  does not change for a strong electrolyte such as chloride over the investigated pH range, variations of the slope  $Z$  can be solely ascribed to changes in the charges of the analyte (pDNA) accessible for ion-exchange. In other words, less charges are accessible on pDNA in the NaCl concentration range below 100 mM as compared to the range above 100 mM (more charges accessible). This behavior can be explained by the effect of salt on solvation of pDNA. At low salt concentration, DNA is strongly solvated and fewer charges are accessible for ion-exchange interaction. High salt concentrations, in contrast, promote the stripping-off of the solvation shell and more charges become accessible on pDNA for ionic interactions with

stationary phase. It further supports the complementarity of the temperature and salt gradient study and, more generally, depicts the great importance of the solvate shell (solvent plus cations) in the chromatographic separation of plasmid DNA.

#### Molecular Recognition Mechanism of Quinine Carbamate Ligand for pDNA Isoforms and Topoisomers.

Common molecular recognition principles for DNA are minor and major groove binding and intercalation. Intercalation as the driving mechanism of binding of the quinine carbamate ligand to DNA was ruled out using AFM imaging of immobilized supercoiled pDNA.<sup>20,21</sup> Interestingly, the ligand features some structural similarities to minor groove binders (e.g., netropsin), such as a H-donor group allowing bifurcated specific hydrogen bonding with AT-rich sequences and geometrically constrained positioning in the groove supported by H-bond mediated ionic interaction (of quinuclidinium moiety) with the phosphate backbone.<sup>17</sup> The results of above thermodynamic study and ionic strength effects are well in agreement with this hypothesis. Supercoiling makes the minor groove better accessible for binding of low molecular ligands,<sup>15</sup> which explains why the supercoiled species are stronger retained than oc and lin isoforms. It is also well-known that the minor groove of B-DNA is strongly solvated.<sup>30</sup> This water shell prevents strong interaction of the ligand in the minor groove of supercoiled pDNA. However, the strong endothermic character of the binding process of the ccc-isoform at elevated temperature indicates that the temperature increase helps to strip off the water shell and makes the minor groove better accessible leading to stronger retention. A qualitatively similar effect can be achieved by increasing the salt concentration which helps as well to strip off the water shell. Though, retention is reduced at increased ionic strength due to disruption of the strong supporting ionic interactions with the phosphate backbone.

The bilinear behavior of the van't Hoff plot can be explained by the particular structure of the hydration shell of pDNA.<sup>31</sup> It is known, for DNA, that strong water clusters are formed around phosphates and donor–acceptor moieties of the base pairs. There is discussed a highly ordered inner hydration shell in the minor groove of natural B-DNA, known as spine of hydration. A second, less-structured hydration shell exists around the phosphate backbone. At low temperature, only the less-ordered water structure might be released upon ligand binding, while at higher temperature also the strongly structured inner solvation shell can be stripped-off allowing ligand-binding into the minor groove. The release of the hydration shell and ions into bulk solvent upon ligand-binding causes a positive change on entropy which leads to lower Gibbs free energy and stronger binding. A similar explanation can be invoked for the ionic strength effect. At low salt concentrations only weakly solvated phosphates might be desolvated, while at higher salt concentration also stronger-bound structured hydration shells can be released. Both good selectivity between ccc and lin/oc isoforms as well as between individual topoisomers can only be accomplished when the inner solvation shell can be stripped off and binding to the minor groove via H-bonds sequences becomes possible. Yet, further experiments are necessary to confirm the identity of the binding moieties and their orientation in order to reveal a detailed picture of the binding process on the molecular level.

**NaCl-Free Elution to Suppress Topoisomer Selectivity.** Later, we have tested NaCl-free chromatography by eluting the pDNA sample from the quinine carbamate column with an organic modifier gradient. Acetonitrile and isopropanol were

used in buffer B, and both resulted in the elution order  $oc < linear < ccc$  ( $T = 50\text{ }^{\circ}\text{C}$ ) and, more importantly, in the cancelation of the topoisomer selectivity. The ccc isoform was eluted at an effective modifier content of 12.9% acetonitrile and 11.7% isopropanol, respectively, hence they possess similar elution strengths (see the Supporting Information for chromatograms). Both, acetonitrile<sup>32</sup> and isopropanol<sup>33</sup> are known to suppress hydrophobic interactions, which in turn must be involved in the binding mechanism, particularly in the interaction with the ccc isoform, because no topoisomer selectivity was observed in this case. Although the chromatographic resolution was reasonable when using isopropanol ( $R_{oc/lin} = 0.25$ ,  $R_{lin/ccc} = 1.17$ ) or acetonitrile ( $R_{oc/lin} = 0.35$ ,  $R_{lin/ccc} = 1.73$ ), we found that pDNA was not eluted quantitatively from the column. A blank run right after a pDNA separation showed a carryover with an area of about 1.5% of the total pDNA area found in the previous chromatogram. However, because the blank chromatogram indicates that the majority of the carryover is due to the oc isoform (see the Supporting Information for the chromatogram), the carryover of this isoform only is 14%. Such a phenomenon on recovery problems of the oc isoform was reported earlier for a commercial anion exchange column,<sup>34</sup> which we especially observed for increasing plasmid sizes.

**pH-Effect on Retention.** We have experienced a carryover of the oc isoform upon elution with an organic modifier gradient and also with a salt gradient. To alleviate the problem, the idea was to use repulsive charge-induced elution. Thus, we studied the effect of buffer pH variation during salt-promoted elution between pH 5 and 8. In general, the retention of all isoforms increased with decreasing pH and below pH 6, the interaction with the stationary phase was already too strong to elute the pDNA completely with 1 M NaCl in buffer B. We noticed a pronounced change in the retention times between pH 6 and 8, which could not be caused by the quinine carbamate ligand per se, since the  $pK_a$  values are  $\sim 10$  for quinuclidine and 4 for the quinoline moiety. However, it was shown earlier by us that the  $\zeta$ -potential of these modified silica particles changes dramatically in this region due to residual silanol groups which render the surface actually zwitterionic with  $pI$ -values around pH 7.5.<sup>35</sup> According to elemental analysis data and as commonly known, only a part of the total number of silanol groups on the particle surface (which is a constant<sup>36</sup>) can be modified by either the ligand or the end-capping group. Therefore, still enough silanols are present to promote silanol–analyte interactions. These negatively charged silanol groups are acting as repulsive electrostatic forces for anionic pDNA above the  $pI$  of the adsorbent surface (see the Supporting Information for surface coverages of used materials). In fact, on an organic polymer support bearing the same quinine carbamate ligand, such pH dependency with pronounced change of the retention around pH 7 was not observed at all. Second, on a diethylaminoethyl (DEAE) carbamate silica column,<sup>17</sup> the plasmid isoforms can be eluted completely from the column at pH 7.9 without NaCl, but on a DEAE-methacrylate-polymer column (both, the commercial DNA-NPR and an in-house produced organomonolithic capillary column<sup>37</sup> after reaction with diethylamine) the plasmids cannot be eluted without NaCl at a pH up to 10 (the highest pH tested). In this context, the silanol activity is dependent on the type of silica that is used as the chromatographic support.<sup>38</sup> Thus, the pH dependency along with the optimal buffer pH value (such allowing the highest isoform resolution) will be

slightly different on each type of silica. For example, the optimum resolution between the plasmid isoforms using a salt gradient on the  $1.5\text{ }\mu\text{m}$  nonporous support is reached at pH 6.0, while on  $5\text{ }\mu\text{m}$  Kromasil silica particles with  $100\text{ }\text{\AA}$  pores, the optimum was around 7.0 due to the shifted  $pI$  of the zwitterionic surface.<sup>35</sup>

**Recovery Problem and Its Solution by pH-Gradient Induced Umpolung of Adsorbent.** The above stated recovery problems are related to eluents with  $pH < pI$  of the adsorbent. In general, recoveries were estimated by comparing the area of the oc isoforms to the linear isoform, which was assumed to elute with full recovery; although a rough estimate, it served accurately enough for our purposes. Molloy et al. estimated that about 50% of the oc isoform of a 6.5 kbp plasmid was not eluting from the commercial DNA-NPR column when compared to agarose gel electrophoresis.<sup>34</sup> We have further experienced that the oc isoform of various plasmids with a size of 10 kbp and above was not eluting at all. However, when using a quinine carbamate silica column with a NaCl- and/or an organic modifier gradient, the oc isoform of the 5 kbp plasmid was fully recovered (i.e.,  $>95\%$ ). Still, for a 10 kbp plasmid we found 60% recovery and for a 15 kbp plasmid the oc form could also be detected (15% recovery), which was a significant improvement already.

In order to obtain full recoveries, a pH gradient seemed to be a promising alternative to the salt gradient. Indeed, we found that a pH gradient from 7.0 to 7.8 leads to full recoveries due to repulsive charge-induced elution and a minimal carryover for oc plasmids up to 15 kbp, the largest plasmid we have tested. With this chromatographic setup we were able to minimize the carryover ( $<2\%$ ). The selectivity and the elution order follow the same trend as described in the previous sections maintaining good isoform separations.

**Switching between Topoisomer Selectivity and Mere Isoform Selectivity.** If the pH gradient is combined with a superimposed salt gradient, (e.g., buffer A, 50 mM sodium phosphate pH 7.0; buffer B, pH 7.8 + 200 mM NaCl,  $60\text{ }^{\circ}\text{C}$ ), the topoisomers of the ccc isoforms can be separated. The resultant chromatogram, however, is not ideally suited for mere isoform separation in process and quality control when there is less interest in the topoisomer pattern. Thus, suppression of topoisomer selectivity is desirable in such cases without compromising isoform resolution. When combining the pH gradient with a superimposed organic modifier gradient (without the addition of NaCl), the topoisomer selectivity is lost and the ccc isoform elutes as a single peak. Because of the excellent selectivity and resolution between the ccc and the linear isoform (as well as the oc form), one could argue that two different modes of interaction must exist, one of which is responsible for isoform separation, the other mode for the topoisomer recognition (see Figure S5 in Supporting Information). However, it is likely that the same chemoaffinity principle, which was derived to be responsible for topoisomer recognition (see colored recognition element in Figure 1c), distinguishes between different isoforms. An indication for this assumption is that ligands which exhibit good topoisomer selectivity<sup>17</sup> show also reasonable isoform selectivity, while ligands with lack of topoisomer recognition also fail to separate isoforms. Concerning the isoform separation, Figure 2b represents a chromatogram recorded under optimized conditions using isopropanol as the organic modifier. Because of its good separation and full recoveries, we consider this method to be most suitable for chromatographic analysis of the true



isoform distribution in a plasmid DNA sample. Improvements will be made in the future concerning the stability of the column, because silica-based materials are not fully stable against cleaning in place by NaOH solution and must be operated well below pH 8, particularly when using elevated temperature.

## CONCLUSION

We have reported on the separation of plasmid DNA isoforms on silica-based columns modified with a quinine carbamate ligand. The van't Hoff plots clearly show that the interaction with this ligand is entropy-driven, which is due to changes in the solvation shell (and possibly the twist of the DNA helix) upon binding to the stationary phase. We identified three types of elution modes, each leading to a different isoform separation: salt, organic modifier, and pH gradient. The salt-mediated elution mode disrupts primarily ionic interactions, such as between the phosphate groups of the DNA backbone and the positively charged quinuclidine moiety of the ligand, and leads to a separation between the oc, linear, and the supercoiled (ccc) topoisomers. Because of carryover effects and incomplete elution of the oc isoform, this mode should be preferably used for topoisomer analysis. The organic modifier-mediated elution mode disrupts primarily hydrophobic interactions, as may be present between the ligand and the grooves of the DNA. The acetonitrile and isopropanol gradient mode cancel the topoisomer selectivity leading to a series of three peaks for each isoform. A pH gradient from pH 7.0 to 7.6 and above changes the charge of the silica surface significantly, and as a consequence, full recoveries of all isoforms and a minimal carryover can be reached independently of the plasmid size. The success of the pH gradient is based on the repulsive interactions between the negatively charged silanol groups and the backbone phosphate groups. A combination of the pH and the organic modifier gradient is the preferred method for analyzing the native isoform distribution in a plasmid sample.

Generally, our results indicate the presence of two binding mechanisms, one of which is of ionic nature, while the other is based on hydrophobic interactions. In order to interact strongly, the (inner) solvate shell of the plasmid DNA needs to be stripped off during the chromatographic (adsorption) process, which is only the case at elevated temperature and apparently facilitated by salt. An indication of the strong contribution of solvation effects are positive changes in entropy upon ligand binding in particular for the ccc form which behaves differently in the high temperature range. By choosing the appropriate mobile phase, the binding mechanism and hence the mode of selectivity can literally be switched. As a result, the true distribution of both, the isoforms and the supercoiled topoisomers can be determined with a single although highly specific column with good recovery.

## ASSOCIATED CONTENT

### Supporting Information

Additional chromatograms, synthesis details,  $\ln k^*$  versus  $\log c$  plot of the salt concentration study, a summary of retention times, and a silanol group coverage table. This material is available free of charge via the Internet at <http://pubs.acs.org>.

## AUTHOR INFORMATION

### Corresponding Author

\*Phone: +49 7071 29 78793. Fax: +49 7071 29 4565. E-mail: [michael.laemmerhofer@uni-tuebingen.de](mailto:michael.laemmerhofer@uni-tuebingen.de).

## Present Address

M.L.: Institute of Pharmaceutical Sciences, Eberhard Karls University Tübingen, Auf der Morgenstelle 8, 72076 Tübingen, Germany.

## Notes

The authors declare no competing financial interest.

## ACKNOWLEDGMENTS

We thank Boehringer-Ingelheim RCV (Vienna, Austria) for financial support as well as for providing the plasmid material. Wolfgang Buchinger and Jochen Urthaler (all Boehringer-Ingelheim RCV) are acknowledged for valuable discussions. Further, we would like to thank Peter Hinterdorfer and co-workers (University of Linz) for support with the atomic force microscopy images.

## REFERENCES

- (1) Schlee, M. *Plasmids for Therapy and Vaccination*; Wiley-VCH: Weinheim, Germany, 2001.
- (2) Yla-Herttuala, S. *Mol. Ther.* **2012**, 20 (10), 1831–1832.
- (3) Doenecke, A.; Krömer, A.; Scherer, M. N.; Schlitt, H.-J.; Geissler, E. K. *J. Gene Med.* **2010**, 12 (10), 810–817.
- (4) Urthaler, J.; Ascher, C.; Woehrer, H.; Necina, R. *J. Biotechnol.* **2007**, 128 (1), 132–149.
- (5) U.S. Department of Health and Human Services Food and Drug Administration Center for Biologics Evaluation and Research. *Guidance for Industry: Considerations for Plasmid DNA Vaccines for Infectious Disease Indications*; Food and Drug Administration, Office of Communication, Training and Manufacturers Assistance: Rockville, MD, 2007.
- (6) Schmidt, T.; Friehs, K.; Schlee, M.; Voss, C.; Flaschel, E. *Anal. Biochem.* **1999**, 274 (2), 235–240.
- (7) Paril, C.; Horner, D.; Ganja, R.; Jungbauer, A. *J. Biotechnol.* **2009**, 141, 47–57.
- (8) Jungbauer, A.; Hahn, R. *J. Chromatogr., A* **2008**, 1184, 62–79.
- (9) Podgornik, A. *J. Sep. Sci.* **2012**, 35 (22), 3059–3072, DOI: 10.1002/jssc.201200387.
- (10) Tarmann, C.; Jungbauer, A. *J. Sep. Sci.* **2008**, 31, 2605–2618.
- (11) (a) Sykora, D.; Svec, F.; Frechet, J. M. J. *J. Chromatogr., A* **1999**, 852 (1), 297–304. (b) Wieder, W.; Bisjak, C. P.; Huck, C. W.; Bakry, R.; Bonn, G. K. *J. Sep. Sci.* **2006**, 29 (16), 2478–2484.
- (12) Onishi, Y.; Azuma, Y.; Kizaki, H. *Anal. Biochem.* **1993**, 210 (1), 63–68.
- (13) Smith, C. R.; DePrince, R. B.; Dackor, J.; Weigl, D.; Griffith, J.; Persmark, M. *J. Chromatogr., B: Anal. Technol. Biomed. Life Sci.* **2007**, 854 (1–2), 121–127.
- (14) Caramelo-Nunes, C.; Tente, T.; Almeida, P.; Marcos, J. C.; Tomaz, C. T. *Anal. Biochem.* **2011**, 412 (2), 153–158.
- (15) Sousa, A.; Sousa, F.; Queiroz, J. A. *J. Sep. Sci.* **2010**, 33 (17–18), 2610–2618.
- (16) Martins, R.; Queiroz, J. A.; Sousa, F. *Biomed. Chromatogr.* **2012**, 26 (7), 781–788.
- (17) Mahut, M.; Lindner, W.; Lämmerhofer, M. *J. Am. Chem. Soc.* **2011**, 134 (2), 859–862.
- (18) Urthaler, J.; Buchinger, W.; Necina, R. *Acta Biochim. Pol.* **2005**, 52 (3), 703–711.
- (19) Morgan, R. D.; Calvet, C.; Demeter, M.; Agra, R.; Kong, H. *Biol. Chem.* **2000**, 381 (11), 1123–1125.
- (20) Mahut, M.; Leitner, M.; Ebner, A.; Lämmerhofer, M.; Hinterdorfer, P.; Lindner, W. *Anal. Bioanal. Chem.* **2012**, 402 (1), 373–380.
- (21) Mahut, M.; Haller, E.; Ghazidezfuli, P.; Leitner, M.; Ebner, A.; Hinterdorfer, P.; Lindner, W.; Lämmerhofer, M. *Angew. Chem., Int. Ed.* **2012**, 51 (1), 267–270.
- (22) Snyder, L. R.; Kirkland, J. J.; Dolan, J. W. *Gradient Elution. In Introduction to Modern Liquid Chromatography*, 3rd ed.; Snyder, L. R.,



Kirkland, J. J., Dolan, J. W., Eds.; John Wiley & Sons: Hoboken, NJ, 2010; pp 430–434.

(23) Haidacher, D.; Vailaya, A.; Horvath, C. *Proc. Natl. Acad. Sci. U.S.A.* **1996**, 93 (6), 2290–2295.

(24) Studdert, D. S.; Patroni, M.; Davis, R. C. *Biopolymers* **1972**, 11 (4), 761–79.

(25) Bates, A. D.; Maxwell, A. DNA supercoiling. In *DNA Topology*, 2nd ed.; Oxford University Press: New York, 2006.

(26) Pulleyblank, D. E.; Shure, M.; Tang, D.; Vinograd, J.; Vosberg, H. P. *Proc. Natl. Acad. Sci. U.S.A.* **1975**, 72 (11), 4280–4284.

(27) Depew, R. E.; Wang, J. C. *Proc. Natl. Acad. Sci. U.S.A.* **1975**, 72 (11), 4275–4279.

(28) Kopaciewicz, W.; Rounds, M. A.; Fausnaugh, J.; Regnier, F. E. *J. Chromatogr., A* **1983**, 266, 3–21.

(29) Hinterwirth, H.; Lämmerhofer, M.; Preinerstorfer, B.; Gargano, A.; Reischl, R.; Bicker, W.; Trapp, O.; Brecker, L.; Lindner, W. *J. Sep. Sci.* **2010**, 33 (21), 3273–3282.

(30) Brovchenko, I.; Krukau, A.; Oleinikova, A.; Mazur, A. K. *J. Am. Chem. Soc.* **2008**, 130 (1), 121–131.

(31) Xie, Y.; Tam, V.; Tor, Y., The Interactions of Small Molecules with DNA and RNA. In *The Chemical Biology of Nucleic Acids*; Mayer, G., Ed. John Wiley & Sons: Chichester, U.K., 2010.

(32) Yang, M.; Fazio, S.; Munch, D.; Drumm, P. *J. Chromatogr., A* **2005**, 1097 (1–2), 124–129.

(33) Khokhlova, T.; Dzyubenko, V.; Berezkin, V.; Bon, A.; Pervov, N.; Shishova, I.; Dubyaga, V.; McHedlishvili, B. *Colloid J.* **2005**, 67 (6), 760–763.

(34) Molloy, M. J.; Hall, V. S.; Bailey, S. I.; Griffin, K. J.; Faulkner, J.; Uden, M. *Nucleic Acids Res.* **2004**, 32 (16), e129/1–e129/10.

(35) Sanchez Munoz Orlando, L.; Hernandez Ever, P.; Lämmerhofer, M.; Lindner, W.; Kennidler, E. *Electrophoresis* **2003**, 24 (3), 390–8.

(36) Zhuravlev, L. T. *React. Kinet. Catal. Lett.* **1993**, 50 (1–2), 15–25.

(37) Preinerstorfer, B.; Bicker, W.; Lindner, W.; Lämmerhofer, M. *J. Chromatogr., A* **2004**, 1044 (1–2), 187–199.

(38) Zhuravlev, L. T. *Colloids Surf., A: Physicochem. Eng. Aspects* **2000**, 173 (1–3), 1–38.

(39) Akasaka, K.; Gyimesi-Forrás, K.; Lämmerhofer, M.; Fujita, T.; Watanabe, M.; Harada, N.; Lindner, W. *Chirality* **2005**, 17 (9), 544–555.

(40) Czerwenka, C.; Lämmerhofer, M.; Maier, N. M.; Rissanen, K.; Lindner, W. *Anal. Chem.* **2002**, 74 (21), 5658–5666.